# Separation in an inclined porous thermogravitational cell

Bilal Elhajjar [a,b], Abdelkader Mojtabi [a,b,*], Pierre Costesèque [a,b], Marie-Catherine Charrier-Mojtabi [c]

[a] Université de Toulouse, INPT, UPS, IMFT (Institut de Mécanique des Fluides de Toulouse), Allée Camille Soula, F-31400 Toulouse, France
[b] CNRS, IMFT, F-31400 Toulouse, France
[c] PHASE, EA 810, UFR PCA, Université Paul Sabatier, 118 route de Narbonne, 31062 Toulouse cedex, France

A B S T R A C T

This paper reports a theoretical and numerical study of species separation in a binary liquid mixture saturating a shallow porous layer heated from below or from above and inclined with respect to the vertical axis. It is shown that the separation can be increased using this configuration and the stability of the unicellular flow obtained in this case is investigated. The critical Rayleigh number obtained is much higher than the one leading to the maximum separation. Experiments performed with a solution of $CuSO_4$ give results which are almost in good agreement with the analytical and the numerical results.

*Keywords:*
Convection
Thermodiffusion
Thermogravitation
Soret effect
Separation
Linear stability

## 1. Introduction

Thermogravitational diffusion is the combination of two phenomena: convection and thermodiffusion. The coupling of these two phenomena leads to species separation. In 1938, Clusius and Dickel [1] successfully carried out the separation of gas mixtures in a vertical cavity heated from the side (thermogravitational column, TGC). During the following years, two fundamental theoretical and experimental works on species separation in binary mixtures by thermogravitation were published. Furry et al. [2] (FJO theory) developed the theory of thermodiffusion to interpret the experimental processes of isotope separation. Subsequently, many works appeared, aimed at justifying the assumptions or extending the results of the theory of FJO to the case of binary liquids [3]. Other works were related to the improvement of the experimental devices to increase separation. Lorenz and Emery [4] proposed the introduction of a porous medium into the cavity. Platten et al. [5] used an inclined cavity, heated from the top, to increase separation. Elhajjar et al. [6] used a horizontal cavity heated from above with temperature gradients imposed on the horizontal walls to improve the separation process with the use of two control parameters. Bennacer et al. [7] suggested splitting the column into three sub-domains in order to increase the separation. The theory developed by Furry et al. [2] for the separation of isotopes in vertical columns differentially heated on the two vertical walls, showed that there is a maximum of separation for an optimal value of the cell thickness. However, in practice, this thickness is of the order of a fraction of mm which significantly reduces the amount of separated species. If we use cells of larger thickness, the separation decreases since the velocity of flow becomes very high in comparison with the velocity leading to the maximum separation. One way to decrease the velocity and to increase the separation is to tilt the cell by a given angle from the vertical. In this case, the horizontal component of the temperature gradient decreases, which decreases the buoyancy force and the velocity of the flow. The tilted cell has already been used by De Groot [3] in the case of bulk fluid but for different forms of the cells.

In this work, an analytical and numerical study of the separation in a porous cell filled with a binary mixture is performed for different inclinations from the vertical axis. Two configurations are considered: cell heated from the top or from the bottom. A linear stability analysis of the unicellular flow leading to separation is presented. Some experiments are also performed in order to corroborate the theoretical and the numerical results.

## 2. Mathematical formulation

In binary fluid mixtures subjected to temperature gradients, the thermodiffusion effect induces a mass fraction gradient. In the expression of the mass flux, $\vec{J}$, of one of the components, in addition to the usual isothermal contribution given by the Fick law,

* Corresponding author at: Université de Toulouse, INPT, UPS, IMFT (Institut de Mécanique des Fluides de Toulouse), Allée Camille Soula, F-31400 Toulouse, France. Tel.: +33 561556793; fax: +33 561558326.
*E-mail address:* mojtabi@imft.fr (A. Mojtabi).

**Nomenclature**

| | |
|---|---|
| $A$ | aspect ratio of the cavity |
| $a^*$ | thermal diffusivity of the mixture $a^* = \lambda^*/(\rho c)_f$ |
| $C$ | mass fraction of the denser component of the mixture |
| $C_i$ | initial mass fraction of the denser component of the mixture |
| $D^*$ | mass diffusion coefficient ($m^2\ s^{-1}$) |
| $D_T^*$ | thermodiffusion coefficient ($m^2\ s^{-1}\ K^{-1}$) |
| $e$ | length of the cavity along the axis $\vec{e}_x$ (m) |
| $k$ | wave number |
| $K$ | permeability of the porous medium ($m^2$) |
| $L$ | length of the cavity along the axis $\vec{e}_z$ (m) |
| $Le$ | Lewis number $Le = a^*/D^*$ |
| $m$ | gradient of mass fraction along the $z$-axis |
| $P$ | pressure of fluid (Pa) |
| $Ra$ | thermal filtration Rayleigh number $Ra = [Keg\beta_T\Delta T(\rho c)_f]/(\lambda^* v)$ |
| $Ra_c$ | critical Rayleigh number associated with transition from equilibrium solution to unicellular flow |
| $S$ | separation |
| $T$ | temperature (K) |
| $t$ | non-dimensional time |
| $\vec{V}$ | velocity of the flow ($m\ s^{-1}$) |
| $u, v$ | velocity components ($m\ s^{-1}$) |

*Greek symbols*

| | |
|---|---|
| $\beta_T$ | thermal expansion coefficient ($K^{-1}$) |
| $\beta_C$ | solutal expansion coefficient |
| $\varepsilon^*$ | porosity of porous medium |
| $\varepsilon$ | normalized porosity |
| $\psi$ | separation ratio $\psi = -(\beta_C/\beta_T)(D_T^*/D^*)C_0(1-C_0)$ |
| $\sigma$ | temporal amplification of perturbation |
| $\lambda^*$ | effective thermal conductivity of the porous medium-mixture system ($W\ m^{-1}\ K^{-1}$) |
| $(\rho c)_f$ | volumetric heat capacity of the mixture ($J\ m^{-3}\ K^{-1}$) |
| $(\rho c)^*$ | effective volumetric heat capacity of porous medium-mixture system ($J\ m^{-3}\ K^{-1}$) |
| $\nu$ | kinematics viscosity of mixture ($m^2\ s^{-1}$) |

*Superscripts and subscripts*

| | |
|---|---|
| nd | non-dimensional |
| 0 | initial value |
| * | equivalent thermophysical properties of the porous medium |

there is an additional contribution proportional to the temperature gradient

$$\vec{J} = -\rho D\vec{\nabla}C - \rho C(1-C)D_T\vec{\nabla}T$$

where $D$ is the mass diffusion coefficient, $D_T$ the thermodiffusion coefficient, $\rho$ the density, and $C$ the mass fraction of the denser component.

We consider a rectangular cell of aspect ratio $A = L/e$ where $L$ is the length of the cell along the axis $\vec{e}_z$ and $e$ is its width along the axis $\vec{e}_x$. The cavity is filled with a porous medium saturated with viscous binary liquid with density $\rho$ and dynamic viscosity $\mu$. The Soret effect is taken into account.

The cavity is inclined at an angle $\alpha$ from the vertical. The gravity vector is $\vec{g} = -g\vec{k}$ where $\vec{k} = -\sin(\alpha)\vec{e}_x + \cos(\alpha)\vec{e}_z$ (Fig. 1). The impermeable walls ($x = 0, x = e$) are kept at different and constant temperatures $T_1$ for $x = 0$ and $T_2$ for $x = e$, with $T_1 < T_2$. The walls ($z = 0, z = L$) are impermeable and insulated. All the boundaries are assumed rigid.

We assume that Darcy's law and the Boussinesq approximation are valid, and that the fluid and the solid phases are in local thermal equilibrium. Dufour effect is neglected as has been done by many authors (see for example [8]) because of its minor influence in liquid mixtures. We set all the properties of the binary fluid constant except the density $\rho$ in the buoyancy term, which depends linearly on the local temperature and the mass fraction:

$$\rho = \rho_0[1 - \beta_T(T - T_0) - \beta_C(C - C_0)] \tag{1}$$

Where $\beta_T$ and $\beta_C$ are the coefficients of thermal and solutal expansion, $\rho_0$ the fluid mixture reference density at temperature $T_0$ and mass fraction $C_0$.

Subject to these constraints, the governing conservation equations for mass, momentum, energy and chemical species are:

$$\begin{cases} \vec{\nabla}.\vec{\mathbf{V}} = 0 \\ \vec{\nabla}P = \rho\vec{g} - \frac{\mu}{K}\vec{\mathbf{V}} \\ (\rho c)^* \frac{\partial T}{\partial t} + (\rho c)_f \vec{\mathbf{V}}.\vec{\nabla}T = \vec{\nabla}.(\lambda^*\vec{\nabla}T) \\ \varepsilon^* \frac{\partial C}{\partial t} + \vec{\mathbf{V}}.\vec{\nabla}C = \vec{\nabla}.\left[D^*\vec{\nabla}C + C(1-C)D_T^*\vec{\nabla}T\right] \end{cases} \tag{2}$$

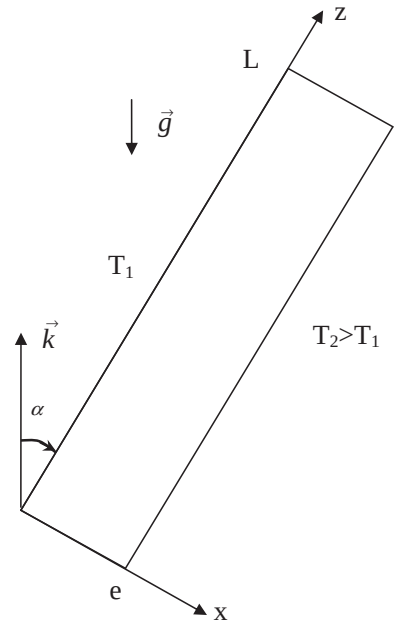


**Fig. 1.** Geometrical configuration of the inclined cell.

We assume that there is little variation in the term $C(1-C)$ of the equation of conservation of species, so we can replace it by $C_0(1-C_0)$, where $C_0$ is the initial mass fraction. The variables are non-dimensionalized with: $e$ for the length, $a^*/e$ for the velocity, $(re^2)/a^*$ for the time, $(\mu a^*)/K$ for the pressure (with $r = (\rho c)^*/(\rho c)_f$, where $(\rho c)^*$ is the effective volumetric heat capacity of the porous medium, and $a^*$ the effective thermal diffusivity of the porous medium), $\Delta T = T_2 - T_1$ for temperature ($T_{nd} = (T - T_1)/\Delta T$) and $\Delta C = \Delta T C_0(1-C_0)D_T^*/D^*$ for the mass fraction ($C_{nd} = (C - C_0)/\Delta C$), where $D_T^*$, $D^*$ are the thermodiffusion and the mass diffusion coefficients of the denser component of mass fraction $C$.

Thus the dimensionless governing conservation equations for mass, momentum, energy and chemical species are:

$$\begin{cases} \vec{\nabla}.\vec{\mathbf{V}} = 0 \\ \vec{\mathbf{V}} = -\vec{\nabla}P + Ra(T-\psi C)[-\sin(\alpha)\vec{e}_x + \cos(\alpha)\vec{e}_z] \\ \frac{\partial T}{\partial t} + \vec{\mathbf{V}}.\vec{\nabla}T = \nabla^2 T \\ \varepsilon\frac{\partial C}{\partial t} + \vec{\mathbf{V}}.\vec{\nabla}C = \frac{1}{Le}(\nabla^2 C + \nabla^2 T) \end{cases} \tag{3}$$

The dimensionless boundary conditions are:

$$\begin{array}{lll} T = 0 & \text{for} & x = 0 \\ T = 1 & \text{for} & x = 1 \\ \frac{\partial T}{\partial z} = -\frac{\partial C}{\partial z} = 0 & \text{for} & z = 0, A \\ \frac{\partial T}{\partial x} = -\frac{\partial C}{\partial x} & \text{for} & x = 0, 1 \\ \vec{V}\cdot\vec{\mathbf{n}} = 0 & \forall M \in \partial\Omega & \end{array} \tag{4}$$

The problem under consideration depends on five non-dimensional parameters: the thermal filtration Rayleigh number $Ra = [Kg\beta_T e\Delta T(\rho c)_f]/(\lambda^* \upsilon)$, the separation ratio $\psi = -(\beta_C/\beta_T)(D_T^*/D^*)\ C_0(1-C_0)$, the Lewis number $Le = a^*/D^*$, the normalized porosity $\varepsilon = \varepsilon^*((\rho c)_f/(\rho c)^*)$ and the aspect ratio $A = L/e$.

## 3. Analytical and numerical results

### 3.1. Analytical results

In the case of a shallow cavity $A \gg 1$, we considered the parallel flow approximation used by Cormack et al. [9]. The basic flow is given as follows:

$$\vec{\mathbf{V}} = W(x)\vec{e}_z; \quad T = bz + f(x); \quad C = mz + g(x) \tag{5}$$

We should have $b = 0$, since constant temperatures are imposed on the walls ($x = 0, 1$).

By replacing $V$, $T$ and $C$ by their expressions (Eq. (5)), and by eliminating the pressure in the system (3) we get the following system:

$$\begin{cases} \frac{dW(x)}{dx} = Ra\left(\frac{df(x)}{dx} - \psi\frac{dg(x)}{dx}\right)\cos(\alpha) - Ra\psi m\sin(\alpha) \\ \frac{d^2 f(x)}{dx^2} = 0 \\ W(x)m = \frac{1}{Le}\frac{d^2 g(x)}{dx^2} \end{cases} \tag{6}$$

By using the boundary conditions for temperature, we obtain:

$$T = x \tag{7}$$

By eliminating $g(x)$ between the first and the third equation of system (6), we obtain the following equation for the velocity:

$$\frac{d^2 W(x)}{dx^2} = -RaLe\psi m\cos(\alpha)W(x) \tag{8}$$

We restrict our study to the case of positive separation ratio ($\psi > 0$). In this case the denser species moves towards the cold wall, *i.e.* the wall ($x = 0$), then the unicellular flow advects this species to the bottom wall, *i.e.* the wall ($z = 0$), so we get a higher mass fraction of the denser species at the bottom of the cavity and therefore $m < 0$.

The angle varies from $-90°$ which corresponds to a horizontal cell heated from above, to $+90°$ corresponding to a horizontal cell heated from below, so $\cos(\alpha)$ is always positive.

Therefore $-RaLe\psi m\cos(\alpha)$ is positive, we assume that $\omega^2 = -RaLe\psi m\cos(\alpha)$, so we get:

$$\frac{d^2 W(x)}{dx^2} = \omega^2 W(x) \tag{9}$$

The solution of Eq. (9) is given by:

$$W(x) = k_1 ch(\omega x) + k_2 sh(\omega x) \tag{10}$$

where $k_1$ and $k_2$ are constants to be evaluated.

To find these constants, we use the following two conditions:

At the stationary state, there is no flow rate through any section perpendicular to the $z$-axis, so: $\int_0^1 W(x)dx = 0$

The first equation of system (6) is valid on the boundaries, so:

$$\left.\frac{dW(x)}{dx}\right|_{x=0} = \left[Ra\left(\frac{df(x)}{dx} - \psi\frac{dg(x)}{dx}\right)\cos(\alpha) - Ra\psi m\sin(\alpha)\right]_{x=0}$$

but for $x = 0$ we have $\frac{\partial C}{\partial x} = \frac{dg(x)}{dx} = -\frac{\partial T}{\partial x} = -\frac{df(x)}{dx} = -1$ so we obtain the following condition for the velocity: $\left.\frac{dW(x)}{dx}\right|_{x=0} = Ra[(1+\psi)\cos(\alpha) - \psi m\sin(\alpha)]$.

Using these two conditions, we find the following expression for the velocity:

$$W(x) = \frac{Ra[(1+\psi)\cos(\alpha) - \psi m\sin(\alpha)][ch(\omega x) - ch(\omega x - \omega)]}{sh(\omega)\omega} \tag{11}$$

This solution is not valid for the limiting cases $\alpha = \pm 90°$. The case $\alpha = 90°$ has been studied in [10,11]. For the case $\alpha = -90°$, the equilibrium solution is infinitely stable.

Once the velocity field has been obtained, we determine the function $g(x)$ using the first equation of system (6). In order to find the constants of integration, we use the equation of conservation of the mass of the denser species:

$\int_0^A \left(\int_0^1 C\,dx\right)dz = 0$ (The integral is equal to zero because the initial dimensionless mass fraction is equal to zero).

By applying these assumptions, we obtain the following expression for the mass fraction:

$$\begin{aligned} C &= -\frac{W(x)}{Ra\cos(\alpha)\psi} + \frac{\cos(\alpha) - \psi m\sin(\alpha)}{\cos(\alpha)\psi}\left(x - \frac{1}{2}\right) - \frac{mA}{2} + mz \\ &= -\frac{[(1+\psi)\cos(\alpha) - \psi m\sin(\alpha)][ch(\omega x) - ch(\omega x - \omega)]}{sh(\omega)\omega\cos(\alpha)\psi} \\ &\quad + \frac{\cos(\alpha) - \psi m\sin(\alpha)}{\cos(\alpha)\psi}\left(x - \frac{1}{2}\right) - \frac{mA}{2} + mz \end{aligned} \tag{12}$$

We still have to determine $m$, so we use the fact that the mass flow of the component having the mass fraction $C$ is zero through any cross section at the stationary state:

$$\begin{aligned} &\int_0^1 (\vec{V}C - \frac{1}{Le}(\vec{\nabla}C + \vec{\nabla}T))\cdot\vec{e}_z dx = 0 \\ &\Rightarrow \int_0^1 \left(W(x)C - \frac{1}{Le}\frac{\partial C}{\partial z}\right)dx = 0 \end{aligned} \tag{13}$$

Since $\int_0^1 W(x)mz\,dx = 0$ we get:

$$\int_0^1 \left(W(x)g(x) - \frac{m}{Le}\right)dx = 0 \tag{14}$$

This leads to a transcendental equation permitting the determination of $m$.

The separation $S$ is defined as the difference of the mass fractions of the denser species between the two ends of the cell ($z = 0$) and ($z = A$): $S = |m|A$.

In the case of a vertical cell ($\alpha = 0°$), and for $Le = 100$ and $\psi = 0.1$, the maximum separation is obtained for $Ra \approx 0.1$ (Fig. 2). For a given binary mixture it is interesting to choose, for the same value of separation, the cell corresponding to the highest value of the Rayleigh number. If we examine Fig. 2, we note that the separation obtained for $\alpha \approx -84°$ and $Ra = 5$ is equal to the maximum separation obtained for $\alpha \approx 0°$ and $Ra = 0.1$. If the temperature difference imposed on the cell is the same for the two previous cases, then the thickness of the cell for $Ra = 5$ would be 50 times greater than that associated with $Ra = 0.1$. Thus for the same degree of separation, the amount of separated species would be higher in the larger cell.

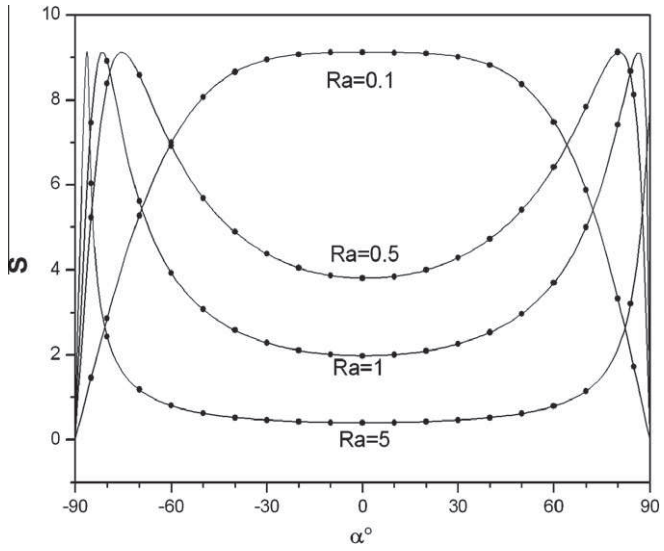


**Fig. 2.** Variation of the separation with the tilt angle for $Le = 100$, $\psi = 0.1$, $A = 20$ and $Ra = 0.1, 0.5, 1, 5$. Solid curves represent the analytical results and the black dots the numerical results.

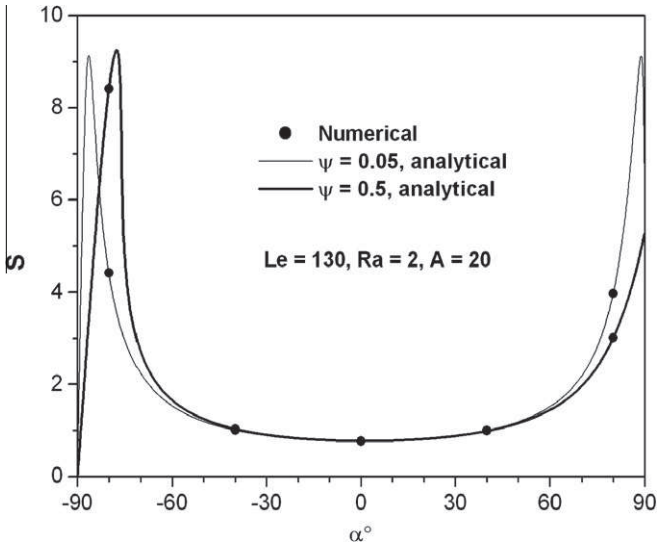


**Fig. 3.** Variation of the separation with the tilt angle for $Le = 130$, $Ra = 2$, $A = 20$, and for $\psi = 0.05, 0.5$.

Fig. 2 shows the variation of separation with the tilt angle for different values of the Rayleigh number and for $Le = 100$ and $\psi = 0.1$.

The cell is heated from above if $\alpha \in [-90°, 0°]$ and from below if $\alpha \in [0°, 90°]$. This figure shows the separation for $Ra = 0.1$ and for Rayleigh numbers that are relatively high in comparison with the optimal Rayleigh number corresponding to the vertical cell ($Ra = 0.5, 1, 5$).

For $Ra = 0.1$, we note that the separation decreases when $\alpha$ varies from 0° to 90° or from 0° to −90°. For $Ra = 0.1$ and in the case of a vertical cell, the coupling between thermodiffusion and convection is optimal. If the cell is inclined from the vertical, the temperature gradient in the $x$ direction remains constant so the influence of thermodiffusion does not change. On the other hand, the horizontal temperature gradient decreases so the intensity of convection decreases and we lose the optimal coupling between thermodiffusion and convection. Also for $Ra = 0.1$, the maximum separation is obtained for $\alpha = 0°$. When $\alpha$ increases, the separation decreases and is zero for $\alpha = 90°$. In the latter case we are dealing with a horizontal cell heated from below, and the critical Rayleigh number of the onset of convection is $Ra_c = 12/(Le\psi)$ (see [10]), which gives for ($\psi = 0.1$, and $Le = 100$) $Ra_c = 12/(100 * 0.1) = 1.2$. This value is greater than 0.1, which means that in this case the equilibrium solution is stable and therefore there is no separation between the ends of the cell. If the angle of inclination decreases from 0°, the intensity of thermodiffusion does not change while the intensity of convection decreases, so the separation decreases and is zero for $\alpha = -90°$. For this position, the cell is horizontal and heated from above with a separation factor $\psi > 0$. For this configuration the equilibrium solution is stable, so there is no flow and then no separation between the two ends of the cell.

For $Le = 100$, $\psi = 0.1$, the value $Ra = 5$ of the Rayleigh number is higher than the value of $Ra$ which gives the maximum separation 0.1 (this value of $Ra$ will be called the "optimal Rayleigh number") for the vertical cell. This value of the Rayleigh number is associated with a thickness of the cell larger than that used for $Ra = 0.1$ for a fixed value of $\Delta T$. We note on Fig. 2 that the separation is much lower for this value of the Rayleigh number in the case of a vertical cell. In order to increase the separation, the cell is inclined from the vertical. If the angle of inclination increases, we see that the separation increases to its maximum value for $\alpha = 90°$. This maximum value is slightly lower than that obtained for $Ra = 0.1$ as, when the cell is tilted, the velocity decreases but does not reach the velocity giving the optimal coupling between convection and thermodiffusion.

If the angle decreases, the separation increases to a maximum value equal to that obtained in the case $Ra = 0.1$, then the separation decreases to zero for $\alpha = -90°$.

For $Ra = 0.5, 1$, the curves of separation have the same shape. If the angle increases the separation increases to reach a maximum and then decreases to 0. For $\alpha = 90°$ the cell is horizontal. The Rayleigh numbers 0.5 and 1 are smaller than the critical Rayleigh number of the onset of convection (1.2); in these conditions there is no separation since there is no flow.

For $Ra = 0.5, 1$, when the angle of inclination varies from 0° to −90°, the separation increases to reach a maximum and then decreases to 0. We note that the optimal angles of inclination are closer to −90° and 90° for $Ra = 1$. In fact, this value of $Ra$ is higher than the value of $Ra$ which gives the maximum separation for the verti-

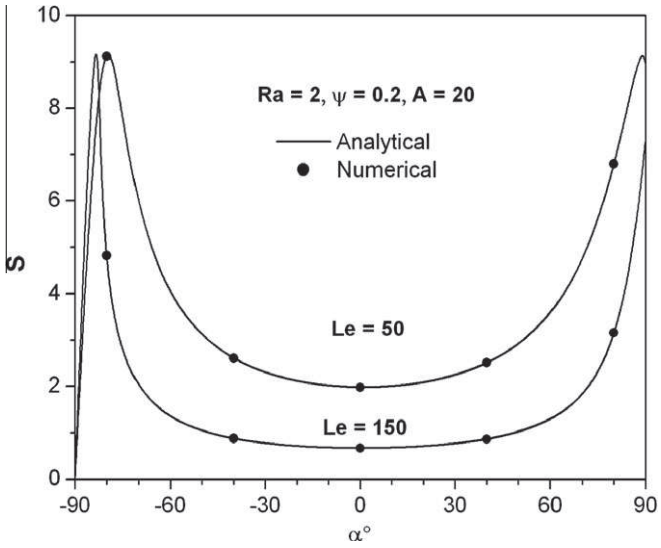


**Fig. 4.** Variation of the separation with the tilt angle for $Ra = 2$, $\psi = 0.2$, $A = 20$, and for $Le = 50, 150$.

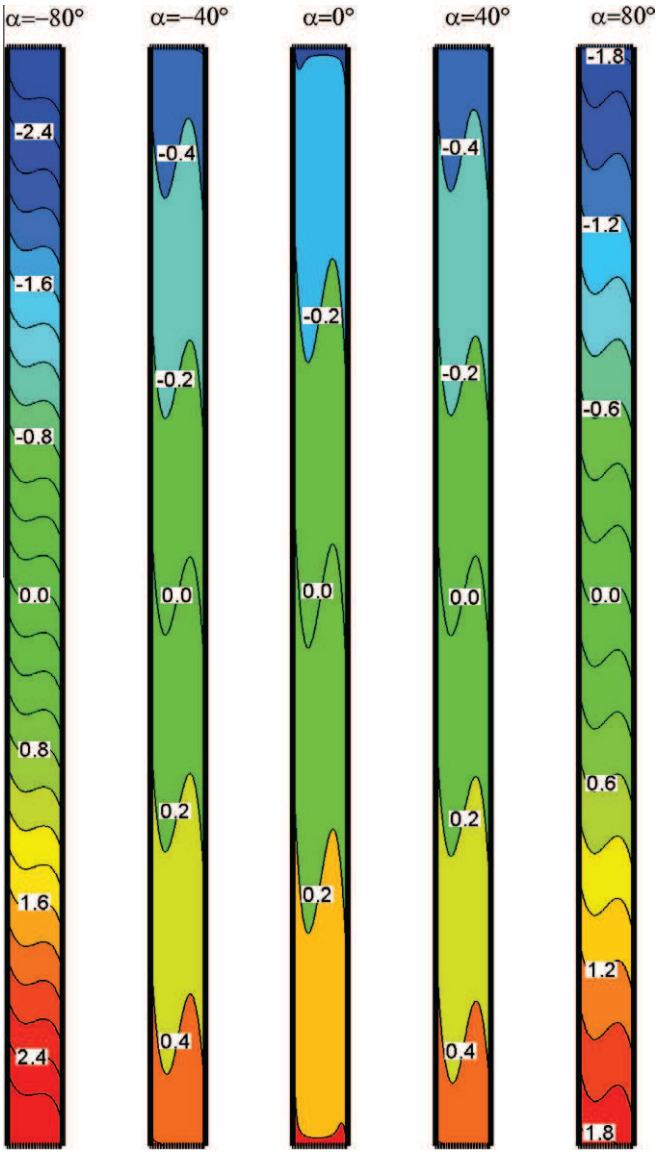


**Fig. 5.** Variation of the mass fraction field with the tilt angle for $Le = 130$, $\psi = 0.2$, $Ra = 2$ and $A = 20$.

cal cell and is higher than 0.5, so the velocity is much higher than that required to obtain maximum separation, so the velocity should be further reduced by tilting the cell to reach the maximum value of the separation.

Fig. 3 shows the variation of separation with the tilt angle for $Le = 130$, $Ra = 2$ and $\psi = 0.05, 0.5$. Fig. 4 shows the variation of separation with the tilt angle for $Ra = 2$, $\psi = 0.2$ and $Le = 50, 150$. Here again we note that the value of the maximum separation is the same in both cases.

### 3.2. Numerical results

In the case of a finite value of $A$, this problem was studied numerically by solving system (3) using a finite element method (using the industrial code COMSOL) and a collocation spectral method [12]. The spatial resolution is $200 \times 30$ for the industrial code and $150 \times 20$ for the collocation method. The numerical results were in good agreement with the analytical ones.

Fig. 5 shows the variation of the mass fraction field with the tilt angle $\alpha$ for a cell of aspect ratio $A = 20$ and for $Le = 130$, $\psi = 0.2$, $Ra = 2$. The black lines show the isoconcentrations and the mass fraction of the denser species is represented using a colored scale.

For $\alpha = 0°$ (vertical cell), the separation is relatively small in comparison with the separations obtained in the case of inclined cells. In the case of a vertical cell, the Rayleigh number $Ra = 2$ is higher than the Rayleigh number leading to maximum separation ($Ra \approx 0.08$), so the velocity is high and the separation is small. When the cell is tilted, the separation increases because, when the cell is inclined, the horizontal component of the thermal gradient decreases and then the velocity of the flow decreases to reach the velocity giving the maximum separation.

We note on this figure that the separation is not similar for the same positive or negative inclination. If $\alpha \in [-90°, 0°]$, the temperature gradient in the $x$ direction has a vertical component and a horizontal one. The horizontal component imposes the magnitude of velocity while the vertical component (cell heated from above) has a stabilizing effect. If $\alpha \in [0°, 90°]$ the temperature gradient in the $x$ direction has a vertical component and a horizontal one, both components imposing the magnitude of the velocity because the cell is heated from below. So in the case of positive inclinations, we should further increase the angle of inclination to obtain lower velocities leading to maximum separation.

## 4. Linear stability analysis of the unicellular flow in an infinite cell heated from below

In the case of a cell heated from below, the unicellular flow (Fig. 5) loses its stability for a relatively low value of Rayleigh number and, in this case, the inclined cell cannot be used for separation. So we will study the stability of the unicellular flow to see if the unicellular flow remains stable for a Rayleigh number higher than the optimal Rayleigh number leading to maximum separation.

Table 1 gives the values of the optimal Rayleigh number for different values of the tilt angle with $\psi = 0.1$ and $Le = 100$. As we can see from this table, the optimal Rayleigh number increases with the angle of inclination. In fact, when $\alpha$ increases at fixed $Ra$, the buoyancy forces decrease and the velocity decreases. Thus in order to maintain the optimal coupling between thermodiffusion and convection, we must increase $Ra$, by increasing $\Delta T$ or $e$.

There are some studies concerning the stability of the unicellular flow in vertical [13–16], or horizontal cells [10,11]. To our knowledge, the linear stability analysis of the unicellular flow obtained in an inclined cell is developed here for the first time. In order to simplify the stability analysis we have adopted the usual assumption used in the case of the vertical cell. We neglect the term $\psi C$ in the momentum transport equation. As has been shown in [17], we observe here that this assumption is valid for the values of the non-dimensional parameter $\psi \in [0.005, 0.5]$ used in our study.

By applying this assumption and solving system (3) with the corresponding boundary conditions and the above mentioned assumptions, we obtain the following expressions for velocity, temperature, and mass fraction fields of the unicellular flow:

**Table 1**
Effect of the tilt angle on the optimal Rayleigh number for $Le = 100$ and $\psi = 0.1$.

| $\alpha$ | $Ra_{opt}$ |
|---|---|
| 60 | 0.19 |
| 65 | 0.24 |
| 70 | 0.27 |
| 75 | 0.35 |
| 80 | 0.48 |
| 85 | 0.80 |

$$\begin{cases} T_0 = x \\ W_0 = Ra\cos(\alpha)(x - 1/2) \\ C_0 = mz + mRa\cos(\alpha)Le(x^3/6 - x^2/4) - x \\ \qquad +[mRa\cos(\alpha)Le]/24 + 1/2 - (mA)/2 \\ m = -(10Lecos(\alpha)Ra)/(Le^2Ra^2\cos^2(\alpha) + 120) \end{cases} \tag{15}$$

In order to investigate the stability of this unicellular flow, it is convenient to rewrite the governing equations using the perturbations of velocity $\vec{\mathbf{v}}$, temperature $\theta$, pressure $p$, and mass fraction $c$:

$$\vec{\mathbf{v}} = \vec{\mathbf{V}} - \vec{\mathbf{V}}_0, \quad \theta = T - T_0, \quad c = C - C_0, \quad p = P - P_0 \tag{16}$$

It is assumed that the perturbation quantities are small and thus the second-order terms can be neglected. We obtain the linear equations where the unknowns are the disturbances.

To take into account more easily the boundary conditions for the temperature and the mass fraction at $x = 0$, 1, we introduce the new variable $\eta = c + \theta$. By developing the disturbances in the form of normal modes $(u, \theta, \eta) = (u(x), \theta(x), \eta(x))e^{ikz+\sigma t}$, we obtain the following system of equations for the perturbations:

$$\begin{aligned} (D^2 - k^2)u &= -ikRa\cos(\alpha)\left[(1+\psi)\frac{d\theta}{dx} - \psi\frac{d\eta}{dx}\right] \\ &\quad + Rak^2\sin(\alpha)[(1+\psi)\theta - \psi\eta] \\ (D^2 - k^2)\theta &= \sigma\theta + u\frac{dT_0}{dx} + ikW_0\theta \\ \frac{ik}{Le}(D^2 - k^2)\eta &= \varepsilon\sigma ik(\eta - \theta) + iku\frac{\partial C_0}{\partial x} - \frac{du}{dx}\frac{\partial C_0}{\partial z} - k^2W_0(\eta - \theta) \end{aligned} \tag{17}$$

where $D = \partial/\partial x$, $k$ is the horizontal wave number, $\sigma = \sigma_r + i\sigma_i$ is the temporal amplification of the perturbation, and $i^2 = -1$.

The corresponding boundary conditions are:

$$u = 0, \quad \theta = 0, \quad \frac{\partial\eta}{\partial x} = 0 \quad \text{for } x = 0, 1 \tag{18}$$

The resulting linear problem is solved by means of a sixth-order Galerkin method, using the following expansions:

$$u = \sum_{i=1}^{N} a_i(x-1)x^i, \quad \theta = \sum_{i=1}^{N} b_i(x-1)x^i,$$

$$\eta = c_1 + c_2(x^2 - 2x^3/3) + \sum_{i=1}^{N-2} c_{i+2}(x-1)^2x^{i+1}$$

We used various methods to determine the critical Rayleigh number: the Galerkin method (method 1), a finite element method to solve the generalized eigenvalue problem (17) and (18) (method 2) and direct numerical simulations (method 3).

Some results of the stability analysis of the unicellular flow are given in Fig. 6.

As we can see from this figure, the critical Rayleigh number has a minimum for a given value of the angle of inclination. The term $\psi C$ was neglected only for the Galerkin method. For the other methods whose results are presented in Fig. 6, we did not adopt this simplification. However the results obtained by these different methods are in good agreement.

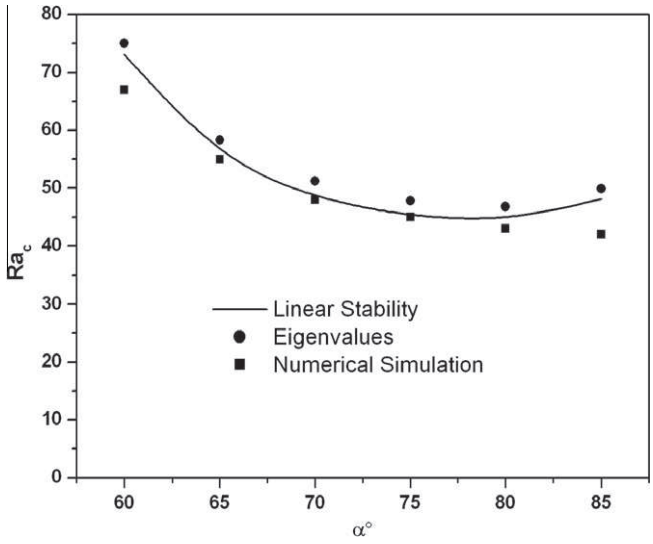


**Fig. 6.** Effect of the tilt angle on the critical Rayleigh number for $Le = 100$ and $\psi = 0.1$.

We also note from this figure that the critical Rayleigh number of the transition from unicellular to multicellular flow is much higher than the one leading to the maximum separation. We conclude that we can use the inclined cell to separate the components of a binary mixture without fearing remixing of the components of the mixture due to instabilities.

Fig. 7 shows the streamlines and the isoconcentrations for $\alpha = 85°$ and for the corresponding optimal Rayleigh number, *i.e.* $Ra = 0.8$. In this case a unicellular flow is observed and we obtain separation between the top and the bottom of the cell.

Fig. 8 shows the streamlines for $Ra = 42$ at the transition from unicellular flow to multicellular flow. For this value of $Ra$ a multicellular flow is obtained and then the inclined cell cannot be used for separation.

## 5. Experiments

We used two types of cells, both of them having two stainless-steel plane boundaries (the plates) maintained at different temperatures in order to create a temperature gradient in a parallelepiped working space. The stainless-steel is chosen to avoid the oxidation observed with $CuSO_4$ mixtures. The dimensions of the first cell ($Cell_1$) (Fig. 9) were 38 cm × 8 cm × 1.5 cm ($A = 25.3$) and of the second one ($Cell_2$) 5.8 cm × 4.4 cm × 0.4 cm ($A = 14.5$). Between the plates, a regular gap $e$ was maintained by a brace made of Plexiglas (thickness $e = 1.5$ cm for $Cell_1$ and $e = 0.4$ cm for $Cell_2$). The temperature at each boundary was kept constant by a regulated water bath. The cells were filled with a porous medium consisting of chemically inert zircon beads (315 μm – 400 μm).

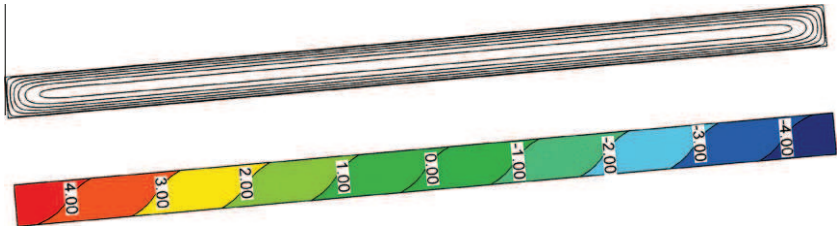


**Fig. 7.** Streamlines and isoconcentrations for $Le = 100$, $\psi = 0.1$, $\alpha = 85°$, $A = 20$ and for the corresponding optimal Rayleigh number $Ra = 0.8$.

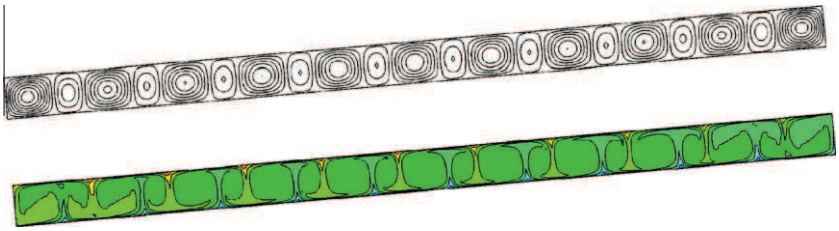

**Fig. 8.** Streamlines and isoconcentrations at the transition between the unicellular and the multicellular flows for $Le = 100$, $\psi = 0.1$, $Ra = 42$, $\alpha = 85°$ and $A = 20$.

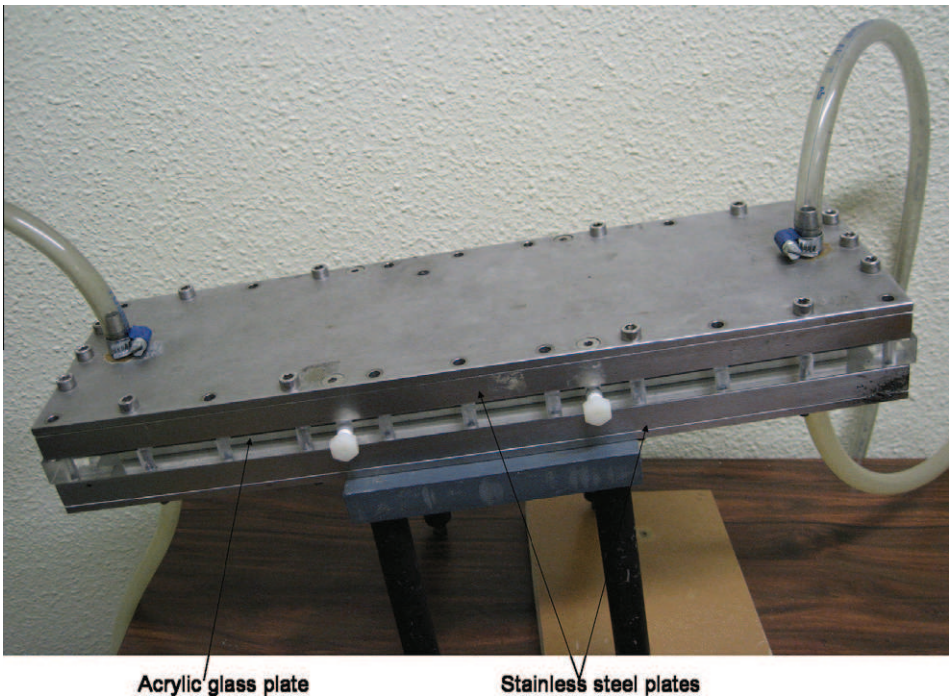


**Fig. 9.** External view of the thermogravitational cell.

We carried out two experiments with the two cells.

The first experiment was with ($Cell_1$) using an aqueous solution of $CuSO_4$ whose concentration expressed as mass fraction was 0.0733. This solution has been studied previously [18,19]. For the presented experiment, we chose an inclination of 75° from the vertical with the cold wall at 10 °C and the hot wall at 30 °C ($Le = 130 \pm 8$, $Ra = 1.500 \pm 0.075$ and $\psi = 0.40 \pm 0.05$).

The experiment lasted 20 days to make sure we reach steady state. The samples were taken at both ends of the cell. The samples were analyzed with a high-resolution refractometer (0.00001). The calibration curve was plotted with the help of solutions prepared at different concentrations. We found a difference of mass fraction $\Delta C_1$ (separation) = $0.0089 \pm 0.0006$ between the two ends of the cell, which corresponds to a relative separation of 12%. For the experiment with the ($Cell_2$), we chose an inclination of −45° from the vertical. The cold wall was kept at 15 °C while the hot wall was at 25 °C ($Le = 130 \pm 8$, $Ra = 0.20 \pm 0.01$ and $\psi = 0.40 \pm 0.05$). The separation $\Delta C_2$ was $0.045 \pm 0.003$ giving a relative separation of 52.8%. This increase in separation is due to the optimal choice of the inclination and the associated value of the Rayleigh number.

These experimental results were compared to the results of 2D numerical simulations under the conditions of the experiment. To conduct the numerical simulation we must know the permeability of the porous medium. To determine the permeability of the porous medium used, several measurements were performed. After repeating the measurements several times using constant head test method, we found a permeability value of $9.2 \times 10^{-11}$ m$^2$ with an accuracy of 2%. The conditions and the results for the two experiments are given in Table 2. As we can see from this table, there is a discrepancy between the experimental and numerical results over 15%. This difference is explained by the difficulty to operate in a porous media (e.g. inaccuracies in measuring the porosity and other thermophysical parameters). The authors who have conducted experimental studies of species separation in vertical thermogravitational columns [19,20] reported errors of the same order of magnitude.

**Table 2**
Comparison between the numerical and the experimental results obtained in the two experimental cells.

| Experiment | Cell | $\Delta T$ | $C_0$ | $\alpha$ (°) | Time of experiment (days) | $\Delta C_{exp}$ | $\Delta C_{num}$ |
|---|---|---|---|---|---|---|---|
| 1 | $Cell_1$ | 20 | 0.0733 | 75 | 20 | $0.0089 \pm 0.0006$ | 0.0105 |
| 2 | $Cell_2$ | 10 | 0.0857 | −45 | 8 | $0.045 \pm 0.003$ | 0.0652 |

## 6. Conclusion

In this paper, analytical and numerical studies have been performed to investigate the separation in a porous cell saturated by a binary liquid mixture and tilted at a given angle with respect to the vertical axis. Most studies dealing with the separation have been concerned with vertical cells. Authors who have examined the case of a tilted cell have restricted their investigations to the cell heated from above.

In this work, we investigated two possibilities: a tilted cell heated from above or from below. This work has shown that the separation can be significantly increased for an optimal value of the tilt angle of inclination. In the first part, an analytical solution was performed in the case of a shallow cavity $A \gg 1$ for different values of the Rayleigh number. The analytical results obtained were corroborated by 2D direct numerical simulations.

In the second part, theoretical and numerical techniques were used to study the stability of the unicellular flow obtained in the case of an inclined cell heated from below. It was observed that there was a minimum value of the critical Rayleigh number for a particular value of the angle of inclination. The direct non-linear numerical simulations performed using a finite element method and a spectral collocation method corroborated the results of the linear stability analysis and allowed the study of the flow structures which appeared after the bifurcation. Experiments performed with a solution of $CuSO_4$ give results which are almost in good agreement with the analytical and the numerical results.

## References


[1] K. Clusius, G. Dickel, Neues verfahren zur gasenmischung und isotroprennung, Naturwisse 6 (1938) 546.

[2] W.H. Furry, R.C. Jones, L. Onsager, On the theory of isotope separation by thermal diffusion, Phys. Rev. 55 (1939) 1083–1095.

[3] S.R. De Groot, Théorie phénoménologique du procédé thermogravitationnel de séparation dans un liquide, Physica 9 (1942) 801–816.

[4] M. Lorenz, A.H. Emery, The packed thermal diffusion column, Chem. Eng. Sci. 11 (1) (1959) 16–23.

[5] J.K. Platten, M.M. Bou-Ali, J.F. Dutrieux, Enhanced molecular separation in inclined thermogravitational columns, J. Phys. Chem. B 107 (42) (2003) 11763–11767.

[6] B. Elhajjar, A. Mojtabi, M. Marcoux, M.C. Charrier-Mojtabi, Study of thermogravitation in a horizontal fluid layer, CR Mecan. 334 (10) (2006) 621–627.

[7] R. Bennacer, A.A. Mohamad, M. El Ganaoui, Thermodiffusion in porous media: multi-domain constituent separation, Int. J. Heat Mass Transfer 52 (2009) 1725–1733.

[8] I.I. Ryzhkov, V.M. Shevtsova, Convective stability of multicomponent fluids in the thermogravitational column, Phys. Rev. E 79 (2009) 1–15. 026308.

[9] D.E. Cormack, L.G. Leal, J. Imberger, Natural convection in a shallow cavity with differentially heated end walls, Part 1, Asymptotic theory, J. Fluid Mech. Digit. Arch. 65 (02) (1974) 209–229.

[10] B. Elhajjar, M.C. Charrier-Mojtabi, A. Mojtabi, Separation of a binary fluid mixture in a porous horizontal cavity, Phys. Rev. E 77 (2008) 1–6. 026310.

[11] M.C. Charrier-Mojtabi, B. Elhajjar, A. Mojtabi, Analytical and numerical stability analysis of Soret-driven convection in a horizontal porous layer, Phys. Fluids 19 (12) (2007) 1–14. 124104.

[12] M. Azaïez, C. Bernardi, M. Grundmann, Spectral method applied to porous media, East–West J. Numer. Math. 2 (1994) 91–105.

[13] D. Henry, H. BenHadid, Multiple flow transitions in a box heated from the side in low-Prandtl-number fluids, Phys. Rev. E 76 (1) (2007) 1–9. 016314, Part: 2.

[14] D. Henry, H. BenHadid, Multiple modes of instability in a box heated from the side in low-Prandtl-number fluids, Phys. Fluids 19 (8) (2007) 1–4. 081702.

[15] A. Zebib, Stability of ternary and binary mixtures in a vertical slot including the Soret effect, J. Chem. Phys. 129 (13) (2008) 1–11. 134711.

[16] A. Zebib, Convective instabilities in thermogravitational columns, J. Non-Equilib. Thermodyn. 32 (2007) 211–219.

[17] M.M. Bou-Ali, O. Ecenarro, J.A. Madariaga, C.M. Santamaria, J.J. Valencia, Thermogravitational measurement of the Soret coefficient of liquid mixtures, J. Phys. – Condens. Matter 10 (15) (1998) 3321–3331.

[18] P. Costesèque, Sur la migration sélective des isotopes et des éléments par la thermodiffusion dans les solutions, Application de l'effet thermogravitationnel en milieux poreux, Observations Expérimentales et conséquences géochimiques, Ph.D. Thesis, Université Paul Sabatier, Toulouse, 1982.

[19] P. Costesèque, T. Pollak, J.K. Platten, M. Marcoux, Transient-state method for coupled evaluation of Soret and Fick coefficients, and related tortuosity factors, using free and porous packed thermodiffusion cells: application to $CuSO_4$ aqueous solution (0.25 M), Eur. Phys. J. E – Soft Matter 15 (3) (2004) 249–253.

[20] Ph. Jamet, D. Fargue, P. Costesèque, G. Marsily, A. Cernes, The thermogravitational effect in porous media: a modelling approach, Transp. Porous Med. 9 (3) (1992) 223–240.